

A biomolecular detection method based on charge pumping in a nanogap embedded field-effect-transistor biosensor

Sungho Kim,¹ Jae-Hyuk Ahn,¹ Tae Jung Park,² Sang Yup Lee,^{2,3} and Yang-Kyu Choi^{1,a)}

¹School of Electrical Engineering and Computer Science, Division of Electrical Engineering, KAIST, Daejeon 305-701, Republic of Korea

²BioProcess Engineering Research Center, Center for Systems and Synthetic Biotechnology, and Institute for the BioCentury, KAIST, Daejeon 305-701, Republic of Korea

³Department of Bio and Brain Engineering, Department of Biological Sciences, and Bioinformatics Research Center, KAIST, Daejeon 305-701, Republic of Korea

(Received 9 April 2009; accepted 12 May 2009; published online 16 June 2009)

A unique direct electrical detection method of biomolecules, charge pumping, was demonstrated using a nanogap embedded field-effect-transistor (FET). With aid of a charge pumping method, sensitivity can fall below the 1 ng/ml concentration regime in antigen-antibody binding of an avian influenza case. Biomolecules immobilized in the nanogap are mainly responsible for the acute changes of the interface trap density due to modulation of the energy level of the trap. This finding is supported by a numerical simulation. The proposed detection method for biomolecules using a nanogap embedded FET represents a foundation for a chip-based biosensor capable of high sensitivity. © 2009 American Institute of Physics. [DOI: 10.1063/1.3148340]

In most cases, the experimentally observed response from FET-type biosensors was only confined as a result of a shift of the flatband voltage (V_{FB}) or the threshold voltage (V_T) that arises from the binding or hybridization of the biomolecules with its complementary part. Im *et al.*¹ evaluated the feasibility of a FET-type biosensor using a nanogap with specific interaction with biotin-streptavidin. Modulation of the gate dielectric constant by means of biomolecular specific binding in the nanogap led to a V_T shift of the transistor, which was used as a sensing parameter. Likewise, Martinez *et al.*² demonstrated another approach in a carbon nanotube FET in which a DNA hybridization produced statistically significant changes in the value of V_T , reflecting the charge trapping characteristic of hybridized DNA. However, the approach of Im *et al.*¹ provided only information to show the change of the gate dielectric constant as a result of a specific binding by monitoring the V_T shift. In addition, the analysis of Martinez *et al.*² only provides information regarding the amount of trapped charge in hybridized DNA using a V_T shift. Therefore, information pertaining to a shift of the flatband or threshold voltage in a FET is limited.

In this paper, a biomolecular detection method in FET-type biosensors is reported. FET has many useful device parameters in addition to V_T . Hence, each device parameter can be utilized as a sensing parameter for detecting biomolecules. One possible device parameter utilized as a sensing parameter is the average density of the interface trap (D_{it}). The interface traps are located between a silicon channel and a gate insulator interface. They represent a very sensitive parameter that can affect the device characteristics. An extraction method related to this parameter, charge pumping, was developed in the 1990s.³⁻⁷ Charge pumping provides information related to the distribution of traps, the energy level of traps, and the amount of trapped charge and the value of D_{it} . A nanogap FET was fabricated in which the gate

insulator was partially etched to form the nanogap. This nanogap exposed the silicon channel to biomolecules directly. Due to the immobilized biomolecules in the nanogap, the interface property of the silicon channel is changed, giving rise to a modulation of D_{it} . Therefore, targeted biomolecules can be electrically detected by charge pumping.

Figure 1(a) shows a cross-sectional view of the proposed nanogap FET device structure as well as the experimental setup for the charge pumping measurement, which is based on a conventional *n*-channel FET. A *p*-type silicon wafer was used as a substrate. For a gate dielectric layer, SiO₂ of 40 nm corresponding to the nanogap height was thermally grown. *n*-type *in situ* doped polycrystalline silicon was deposited and patterned for a gate electrode. The source and drain were formed by ion implantation and subsequent thermal activation. The gate insulator (SiO₂) was then etched using a buffered oxide etchant to form the nanogap underneath the polysilicon gate. The length of the nanogap was 250 nm, as

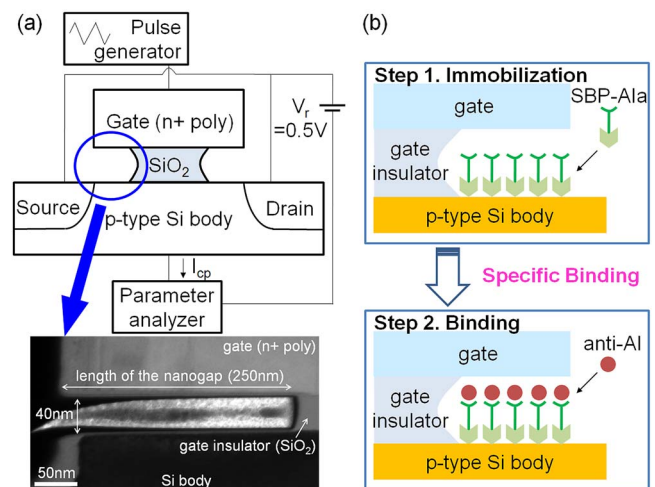


FIG. 1. (Color online) (a) Schematic of a fabricated nanogap FET and experimental set-up of the charge pumping measurement, and a transmission electron microscopy image of the nanogap embedded FET (b) Schematic representation of the antigen-antibody binding of AI in the nanogap.

^{a)}Author to whom correspondence should be addressed. Electronic mail: ykchoi@ee.kaist.ac.kr.

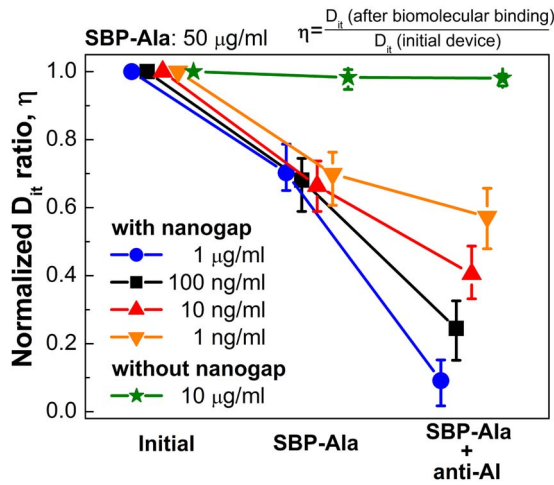


FIG. 2. (Color online) (a) The D_{it} values of nanogap FET devices undergoing SBP-AIa and antiAI immobilization. Each data point was extracted from 20 different devices, and the total number of devices is 100. The modulation of D_{it} depends on the concentration of specific binding between SBP-AIa and antiAI. A control experiment using a FET device without a nanogap indicates that only bounded biomolecules in the nanogap can modulate D_{it} .

controlled by the wet-etching time. The width and gate length of the nanogap FET was 10 μm and 2 μm , respectively. To measure the charge pumping current (I_{cp}), the source and drain of the transistor were connected and sustained at a reverse bias ($V_r=0.5$ V) voltage with respect to the substrate.⁷ When a pulse was applied into the gate electrode, the state of the transistor was switched between the inversion mode and the accumulation mode repeatedly. Consequently, electrons trapped in the interface traps in the inversion mode recombined with holes from the substrate in the accumulation mode. This electron-hole recombination gave rise to a current flow from the substrate to the channel, I_{cp} . D_{it} can be described by the equation

$$I_{cp} = f \cdot A_G \cdot q^2 \cdot D_{it} \cdot \Delta\psi_s,$$

where $\Delta\psi_s$ is the total sweep of the surface potential, f is the frequency of the applied pulse, and A_G is the device area. From this equation, it can be simply concluded that D_{it} is proportional to I_{cp} . In this work, D_{it} was extracted from the I_{cp} measurement, as in the work of Groeseneken *et al.*⁷

To demonstrate the effectiveness of the proposed nanogap FET as a biosensor, the antigen-antibody binding of avian influenza (AI) was used. For the immobilization of the AI surface antigen (AIA) in the nanogap, the silica-binding protein (SBP)-AIa fusion protein was designed. As shown in Fig. 1(b), the SBP part of the fusion protein serves as an anchoring domain onto the silica surface, exploiting the silica-binding affinity of the domain, whereas the AIA part is a specific recognition element for the anti-AI antibody. It should be noted that after the nanogap etching process, native oxide was grown inside the nanogap surface and on the entire device surface because the device was exposed to air ambient. Therefore, SBP-AIa was immobilized on the entire device surface as well as in the nanogap. To immobilize SBP-AIa, the nanogap FET was immersed in SBP-AIa dissolved in a phosphate-buffered saline (PBS, pH 7.4) solution for 1 h. Thereafter, for specific binding of the antigen-antibody AI, the device was immersed again in an antiAI/PBS solution for 1 h.

Figure 2 shows the modulation of D_{it} in a nanogap FET

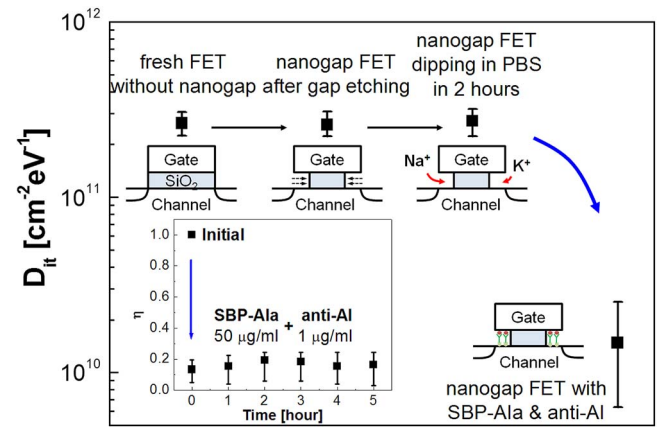


FIG. 3. (Color online) The modulation of D_{it} in three different groups: a fresh FET device without a nanogap, a FET with a nanogap, and a FET with a nanogap after dipping in PBS. Each data point was extracted from 20 different devices. The inset figure shows the normalized D_{it} ratio as a function of time.

in a comparison made before and after the binding of SBP-AIa and anti-AI. When the concentration of the SBP-AIa solution was fixed at 50 $\mu\text{g/ml}$, the modulation of D_{it} depends on the anti-AI concentration. The concentrations of anti-AI solution used here ranged from 1 $\mu\text{g/ml}$ to 1 ng/ml. As shown in Fig. 2, D_{it} decreased due to the immobilization of the SBP-AIa into the nanogap. In addition, it decreased more after the specific binding between SBP-AIa and anti-AI. Using the charge pumping method, sensitivity can fall below the 1 ng/ml concentration regime and sensitivity can be maintained stably more than 5 h, as shown in the inset of Fig. 3.

To confirm that the measured electrical signals indeed originated from biomolecules in the nanogap, a series of control experiments was performed. First, it was confirmed whether or not immobilized biomolecules onto the entire device surface except inside the nanogap can modulate D_{it} . To verify this, the same biomolecular detection procedure was performed using a FET without a nanogap as a control group. As shown in Fig. 2, in the case of the FET without the nanogap, there was no modulation of D_{it} . This is a natural result in that the charge pumping method is an extraction method for the interface property between a silicon channel and a gate insulator. Accordingly, only a small fraction of the biomolecules immobilized in the nanogap with an exposed silicon channel can modulate D_{it} ; immobilized biomolecules onto the other device surface cannot affect the interface property. Stable electrical measurement results statistically were provided in that only a slight fluctuation of data among devices was shown. This is in contrast with the severe fluctuation when using the V_T shift measurement method.^{1,2} Second, it was verified that the modulation of D_{it} did not arise from the mobile ions of K^+ and Na^+ that were included in the PBS but instead originated from the biomolecules. Three different groups were prepared: a fresh FET without a nanogap, a nanogap FET, and a nanogap FET after dipping in PBS. Figure 3 shows that only negligible modulation of D_{it} was observed in the nanogap FET case and in the nanogap FET after dipping in the PBS case. These findings indicate that the modulation of D_{it} did not originate as a result of the mobile ions in the PBS solution. Next, Fig. 4 shows the result of a false-positive test as conducted to verify the selectivity. It is known that the binding between SBP and silica

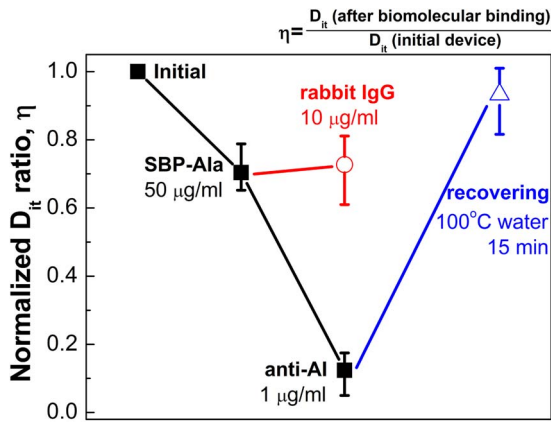


FIG. 4. (Color online) Comparative results for the antigen-antibody binding of AI: recovery test in which the SBP-silica binding is broken, and a false-positive test using rabbit IgG. Each data point was extracted from 20 different devices.

is efficiently broken by nonionic aqueous solutions upon brief exposure to high temperatures.⁸ To confirm this phenomenon, nanogap FETs with bound biomolecules were immersed in hot de-ionized water (100 °C) for 15 min and were then washed several times using deionized water. As shown in Fig. 4, D_{it} was reversibly recovered to its original value in a fresh state. This experiment shows that the modulation of D_{it} resulted from the biomolecules immobilized in the nanogap. Moreover, for a false-positive test, nonspecific binding of rabbit immunoglobulins (IgG) was used for SBP-AIa. Due to the nonspecificity between SBP-AIa and the rabbit IgG, D_{it} remained unchanged. Therefore, the nanogap FET biosensor using the charge pumping method could effectively detect targeted biomolecules.

The decrease of D_{it} likely occurred because the biomolecules immobilized in the nanogap provided extra interface states or modulated the energy level of the trap. If biomolecules provide deep-level traps, trapped electrons cannot recombine with holes easily in the accumulation mode. Consequently, this leads to a decrease of I_{cp} (It should be noted that I_{cp} is proportional to D_{it}). In contrast, if biomolecular bindings act as a shallow-level trap, trapped electrons traps easily recombine, leading to an increase of I_{cp} . Therefore, antigen-antibody binding of AI can be assumed as deep-level traps. To verify these assumptions, a numerical simulation was carried out.^{9,10} Figure 5(a) shows a schematic of a nanogap FET device structure and the assigned trap energy level distributions used in the simulation. Different energy levels of the interface trap distribution are specified in the nanogap region. To assign the shallow-level traps in the nanogap, the distribution of the acceptor-type interface states in the forbidden bandgap is centered at 0.2 eV above the silicon valence band maximum ($E_v+0.2$ eV). In addition, the donor-like distribution is centered at 0.2 eV below the silicon conduction band minimum ($E_c-0.2$ eV). These traps are distributed across the bandgap in a delta-function-like manner. On the other hand, in the case of deep-level traps in the nanogap, both acceptor-type and donor-type interface states are located near the intrinsic Fermi-level of the bandgap. Interface states of the channel region apart from the nanogap are defined as low-density shallow level traps. Figure 5(b) shows the time-evolution of I_{cp} when the gate was pulsed

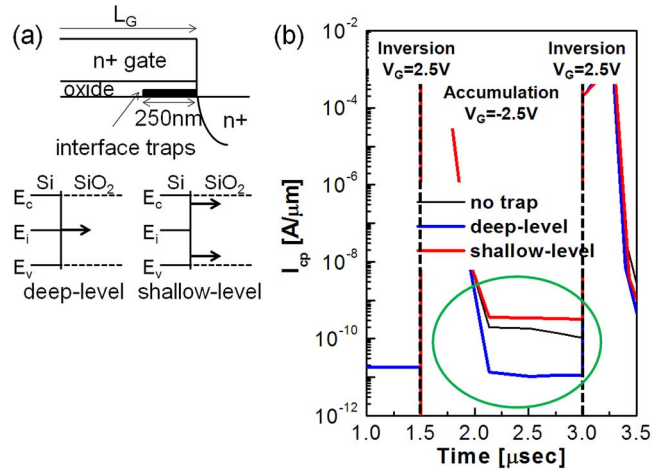


FIG. 5. (Color online) (a) Schematic of the nanogap FET device structure and assigned trap energy level distributions in the nanogap region used for the simulation. Interface states of the channel region except the nanogap are defined as low-density shallow-level traps. (b) The time-evolution of the value of I_{cp} when the gate is pulsed from the accumulation mode ($V_G=-2.5$ V) to the inversion mode ($V_G=2.5$ V) and back again to -2.5 V with different levels of interface states.

from -2.5 V (accumulation mode) to 2.5 V (inversion mode) and back again to -2.5 V with different energy levels of interface states. Figure 5(b) shows that as the shallow-level traps are located in the nanogap, a greater value of I_{cp} is generated compared to cases in which traps are not located in the nanogap. On the other hand, deep-level traps in the nanogap lead to decrease the value of I_{cp} . Therefore, it can be concluded that a different energy level of the interface trap can modulate D_{it} and that the antigen-antibody bindings of AI can be regarded as deep-level traps. This simulation result is consistent with the measured one.

This research was supported by a Grant No. 08K1401-00210 from the Center for Nanoscale Mechatronics & Manufacturing, one of the 21st Century Frontier Research Programs supported by the Korea Ministry of Education, Science and Technology (MEST). It was also partially supported by the National Research and Development Program (Grant No. 2005-01274) for the development of biomedical function monitoring biosensors, sponsored by the NRL program of KOSEF (Grant. No. R0A-2007-000-20028-0).

¹H. Im, X.-J. Huang, B. Gu, and Y.-K. Choi, *Nat. Nanotechnol.* **2**, 430 (2007).

²M. T. Martinez, Y.-C. Tseng, N. Ormategui, I. Loinaz, R. Eritja, and J. Bokor, *Nano Lett.* **9**, 530 (2009).

³M. Tsuchiaki, H. Hara, T. Morimoto, and H. Iwai, *IEEE Trans. Electron Devices* **40**, 1768 (1993).

⁴Y. Maneglia and D. Bauza, *J. Appl. Phys.* **79**, 4187 (1996).

⁵P. Heremans, J. Witters, G. Groeseneken, and H. E. Maes, *IEEE Trans. Electron Devices* **36**, 1318 (1989).

⁶M. G. Ancona, N. S. Saks, and D. McCarthy, *IEEE Trans. Electron Devices* **35**, 2221 (1988).

⁷G. Groeseneken, H. E. Maes, N. Beltran, and R. F. D. Keersmaecker, *IEEE Trans. Electron Devices* **31**, 42 (1984).

⁸A. Holmberg, A. Blomstergren, O. Nord, M. Lukacs, J. Lundeberg, and M. Uhlén, *Electrophoresis* **26**, 501 (2005).

⁹G. S. Samudra, A. Yip, and L. K. See, *IEEE International Conference on Semiconductor Electronics (ICSE)*, Bangi, Malaysia, 24–26 November 1998 (IEEE, New York, 1998), p. 32.

¹⁰Medici User Guide, Version Z-2007.03, March 2007, SYNOPSIS.